

# Journal of Pharmacognosy and Phytochemistry

Available online at www.phytojournal.com



E-ISSN: 2278-4136 P-ISSN: 2349-8234 Impact Factor (RJIF): 6.35 www.phytojournal.com JPP 2025; 14(5): 398-406

JPP 2025; 14(5): 398-40 Received: 27-06-2025 Accepted: 29-07-2025

#### Eda Sönmez Gürer

Department of Pharmacognosy, Faculty of Pharmacy, Sivas Cumhuriyet University, Sivas, Turkey

#### **Emre Can Buluz**

Department of Biotechnology, Institute of Science, Ege University, Izmir, Turkey

#### Savaş Kaya

Department of Chemistry, Faculty of Science, Sivas Cumhuriyet University, Sivas, Turkey

# Integrated in silico analysis of *Rosa canina* phytochemicals targeting tyrosinase: Molecular docking, ADME, and toxicity predictions

# Eda Sönmez Gürer, Emre Can Buluz and Savaş Kaya

**DOI:** https://www.doi.org/10.22271/phyto.2025.v14.i5e.15601

#### Abstract

Rosa canina is a medicinal plant rich in phenolics, flavonoids, and vitamins with antioxidant, antiinflammatory, and dermatoprotective effects. In this study, twenty-five phytochemicals were retrieved
from Dr. Duke's Database and optimized using Avogadro. Tyrosinase crystal structure was prepared in
UCSF Chimera, and molecular docking was performed with PLANTS in a defined pocket. Interactions
were analyzed in BIOVIA Discovery Studio, followed by ADME profiling with SwissADME and
toxicity assessment via ProTox 3.0. Docking showed linoleic acid, alpha-tocopherol, and oleic acid had
the best affinities, stabilized by hydrogen bonding and hydrophobic contacts with catalytic residues
(His53, His189, His193, Arg54). ADME predictions indicated high gastrointestinal absorption for fatty
acids and vitamins, but poor absorption and drug-likeness violations in glycosylated flavonoids. Toxicity
predictions revealed most compounds were non-mutagenic and non-cytotoxic, though nephrotoxicity
appeared in polyphenols. Linoleic and oleic acids displayed the most favorable overall safety.

Keywords: ADME, molecular docking, Rosa canina, toxicity analysis, tyrosinase

#### Introduction

In recent years, the growing popularity of herbal remedies has led to an increasing number of studies on various plants traditionally used in medicine. One of the important plants used in traditional medicine is Rosa canina. Rosa canina, commonly known as rosehip, is a widely distributed species in the Rosaceae family. Its fruit and seeds are particularly rich in bioactive phytochemicals, including flavonoids (e.g., (+)-catechin, (-)-epicatechin, hyperoside, astragalin, rutin), phenolic acids (e.g., gallic, ellagic, ferulic, caffeic acids), and vitamins such as vitamin C and E, which confer notable antioxidant, anti-inflammatory, and dermatoprotective properties [1,2]. The weight of a rose hip and seed is between 1.25 and 3.25 grams. Out of this weight, 71% is the pericarp, and about 29% is the seed [3]. The chemical composition of Rosa canina varies according to factors such as cultivar, growing region, climate, maturity, cultivation practices, and storage conditions [2]. In vitro studies have demonstrated that extracts from Rosa canina notably water- and enzyme-assisted extracts of rosehip fruits exhibit considerable tyrosinase inhibitory activity, with one study reporting up to 80% inhibition under optimized extraction conditions [4]. Additionally, isolates from Rosa canina roots, including (+)-catechin, have shown anti-tyrosinase activity in combination with anti-collagenase and antioxidant effects [5]. In the context of skin health and pigmentation, several studies link high total phenolic content (TPC) and total flavonoid content (TFC) from Rosa canina extracts to significant tyrosinase inhibitory activity. For example, an in vitro study using ultrasonic extraction of Rosa canina pseudo-fruits uncovered a strong positive correlation between TPC or TFC and tyrosinase inhibition. The most phenolic-rich extracts also showed robust antioxidant potential, which correlated with enhanced inhibitory effects on the tyrosinase enzyme [6].

Tyrosinase is a copper-containing oxidase that plays a critical role in melanin biosynthesis by catalyzing both the hydroxylation of monophenols and the oxidation of o-diphenols to o-quinones the rate-limiting reactions in the Raper-Mason pathway of melanogenesis <sup>[7]</sup>. It catalyzes two essential and rate-limiting reactions in the Raper-Mason pathway: the orthohydroxylation of monophenols such as L-tyrosine to L-DOPA (monophenolase activity) and the subsequent oxidation of L-DOPA to dopaquinone (diphenolase activity) <sup>[8]</sup>. Tyrosinase is named after its primary substrate, tyrosine. While the enzyme exhibits broad substrate specificity in both of its activities, it demonstrates a stronger affinity for the L-isomers compared to the corresponding D-isomers <sup>[9]</sup>. Because excessive tyrosinase activity contributes

Corresponding Author: Eda Sönmez Gürer Department of Pharmacognosy, Faculty of Pharmacy, Sivas Cumhuriyet University, Sivas, Turkey

hyperpigmentation and associated dermatological conditions, the search for effective and safe tyrosinase inhibitors has been a significant focus in both cosmetic and pharmaceutical research [10]. In addition to its biomedical relevance, tyrosinase also plays a central role in the enzymatic browning of fruits and vegetables, a major cause of postharvest losses in the food industry, thereby underscoring its importance as a biotechnological target [11]. Although several synthetic inhibitors, such as hydroquinone, kojic acid, and arbutin, have been widely used, their applications are limited due to side effects including cytotoxicity, instability, or potential carcinogenicity [12, 13]. As a result, growing attention has shifted toward natural phytochemicals particularly polyphenols and flavonoids because of their structural diversity, safety profiles, and ability to interact with the active site of tyrosinase through multiple binding modes [14].

Recent advances in computational approaches such as molecular docking, pharmacokinetic modeling, and in silico toxicity prediction have further accelerated the screening of large phytochemical libraries, enabling the identification of promising candidates with high binding affinity and favorable ADME-toxicity characteristics before experimental validation [15]. Molecular docking is widely employed to model proteinligand interactions and to estimate the binding affinity of bioactive compounds toward specific targets such as tyrosinase [16]. When complemented with pharmacokinetic modeling tools like SwissADME [17] and toxicity prediction platforms such as ProTox 3.0 web server [18], in silico pipelines can provide a comprehensive evaluation of compound drug-likeness and safety at an early stage of research. Such integrative computational strategies not only accelerate the identification of promising lead candidates but also minimize attrition rates in subsequent experimental validation by filtering out molecules with poor ADME or unfavorable toxicity profiles. In the context of Rosa canina, this combined approach has the potential to uncover novel phytochemicals with strong tyrosinase inhibitory capacity and favorable pharmacological attributes, thereby contributing to the development of safer and more effective agents for cosmetic and therapeutic management of hyperpigmentation disorders.

This study aimed to comprehensively investigate phytochemicals from *Rosa canina* as potential tyrosinase inhibitors by employing an integrated *in silico* strategy that combined molecular docking, pharmacokinetic (ADME) evaluation, and toxicity prediction, with the aim of identifying candidates that exhibit both high binding affinity and favorable safety profiles for subsequent experimental validation.

#### **Materials and Methods**

#### Preparation of protein and active phytochemicals

Twenty-five active phytochemicals of *Rosa canina* were retrieved from Dr. Duke's Phytochemical and Ethnobotanical Databases <sup>[19]</sup>, a well-established resource that compiles comprehensive information on phytochemicals, their biological activities, and ethnobotanical relevance. The three-dimensional chemical structures of the molecules were obtained from the PubChem database <sup>[20]</sup>, and their geometries were subsequently optimized using the Avogadro software <sup>[21]</sup>. To obtain energetically favorable conformations suitable for docking studies, geometry optimization was carried out employing the Universal Force Field (UFF), which is commonly applied for small organic molecules due to its reliability in reproducing accurate conformational energies.

Following optimization, each structure was saved in mol2 file format, ensuring compatibility with molecular docking. For the protein target, the three-dimensional crystal structure of tyrosinase (PDB ID: 1WX2) [22] was obtained from the Protein Data Bank (PDB) [23]. This structure was selected due to its high resolution and frequent use in computational studies investigating tyrosinase inhibitors. Prior to molecular docking, the protein structure was processed using UCSF Chimera [24]. Pre-processing steps included the removal of crystallographic water molecules, non-essential ligands, and ions that may interfere with the binding analysis. Hydrogen atoms were added to the protein structure to correct valence states, and missing side chains or loops were repaired where necessary using the built-in Dock Prep module. Finally, the protein saved in mol2 format for subsequent docking.

#### Molecular docking

Molecular docking studies were performed using the PLANTS (Protein-Ligand ANT System) [25] software to predict the binding conformations and affinities of the selected active molecules from Rosa canina against the target protein (PDB ID: 1WX2). The binding pocket was defined according to the catalytic pocket coordinates set as x = -12.27, y = -13.17, and z = 18.07. Docking calculations were carried out under default scoring and search parameters of PLANTS, which employ an ant colony optimization algorithm to efficiently explore ligand conformational space and rank the binding poses according to predicted affinity. The resulting docking poses for each ligand were subsequently visualized and analyzed using BIOVIA Discovery Studio Visualizer [26], where both two-dimensional (2D) and three-dimensional (3D) interaction diagrams were generated. These analyses enabled the identification of key hydrogen bonds, hydrophobic contacts, electrostatic interactions, and  $\pi$ - $\pi$  stacking interactions between the ligands and the amino acid residues of the binding pocket, thereby providing a comprehensive understanding of the binding modes and molecular recognition features of the studied compounds.

### **ADME** analysis

Following the molecular docking analysis, the twenty-five active molecules were subjected to pharmacokinetic and druglikeness evaluations using the SwissADME web tool. The canonical SMILES strings of the molecules were generated and uploaded to the platform to predict their physicochemical profiles, descriptors, lipophilicity solubility, pharmacokinetic properties. Specifically, gastrointestinal (GI) absorption and blood-brain barrier (BBB) permeability were assessed to estimate the oral bioavailability and central nervous system (CNS) penetration potential of the active molecules. In addition, cytochrome P450 (CYP) isoform inhibition profiles were analyzed to identify potential drugdrug interaction risks. Lipinski's rule of five, Veber's rule, and other drug-likeness filters were applied to evaluate the molecules' compliance with established criteria for oral drugs. Furthermore, bioavailability scores and synthetic accessibility indices were calculated to provide insights into the feasibility of the compounds as lead drug candidates.

### **Toxicity prediction**

Following the ADME evaluation, the twenty-five active molecules were subjected to toxicity prediction using the ProTox 3.0 web server, a widely utilized computational tool for *in silico* toxicological profiling. Each molecule was uploaded in SMILES format into the server interface, which subsequently predicted multiple toxicological endpoints based

on machine learning models trained on large experimental datasets. Specifically, ProTox 3.0 web server provided predictions for oral toxicity (LD50 values), hepatotoxicity, immunotoxicity, mutagenicity, cytotoxicity, carcinogenicity, alongside the classification of molecules into Globally Harmonized System (GHS) hazard classes. In addition, the tool estimated potential interactions with known toxicological pathways, allowing a deeper understanding of possible adverse effects. The toxicity class ranking (ranging from Class I, highly toxic, to Class VI, non-toxic) was recorded for each molecule, and the predicted probability scores were considered to assess the reliability of the outcomes. This comprehensive in silico analysis enabled the identification of candidate molecules with a favorable safety profile, thereby narrowing down the pool of active compounds for further consideration in downstream drug development pipelines. This comprehensive in silico analysis enabled the identification of candidate molecules with a favorable safety profile.

# **Results and Discussion**

#### Molecular docking analysis

Molecular docking studies have shown the interaction of twenty-five active molecules obtained from Rosa canina with tyrosinase enzyme. Molecular docking studies are used to determine the binding energy between the enzyme and the molecules under study. The enzyme's crystal structure is selected from the Protein Data Bank. Table 1. shows the binding energies obtained from molecular docking analysis of twenty-five active molecules with tyrosinase. The molecular docking analysis of twenty-five phytochemicals from Rosa canina against tyrosinase (PDB ID: 1WX2) revealed a broad spectrum of binding affinities, as reflected in their docking scores. Among the tested molecules, linoleic acid (-89,79 kcal/mol), alpha-tocopherol (-89,58 kcal/mol), oleic acid (-83,82 kcal/mol), thiamin (-82,61 kcal/mol), and hyperoside (-81,13 kcal/mol) exhibited the most favorable docking scores, indicating strong binding interactions with the binding pocket of tyrosinase.

Table 1: Predicted binding scores of active molecules with tyrosinase enzyme.

Molecule Name	Docking Score (kcal/mol)				
Acetic acid	-46,96				
Alpha tocophenol	-89,58				
Protocatechuic acid	-65,85				
Quercitrin	-79,80				
Riboflavin	-73,34				
Tannin	1600,21				
Thiamin	-82,61				
Vanillic acid	-62,86				
Vanillin	-60,44				
Ascorbic acid	-64,42				
Beta carotene	556,88				
Caffeic acid	-66,87				
Catechin	-70,73				
Citric acid	-63,75				
Epicatechin	-71,49				
Ferulic acid	-66,31				
Gallic acid	-67,14				
Hyperoside	-81,13				
Isoquercitrin	-79,10				
Lecithin	134,48				
Linoleic acid	-89,79				
Oleic acid	-83,82				
P-coumaric acid	-63,43				
Niacin	-57,32				
Pectin	-65,06				

In contrast, acetic acid (-46.96 kcal/mol), niacin (-57,32 kcal/mol), and vanillin (-60,44 kcal/mol) showed weaker binding affinities, which is consistent with their limited functional groups available for strong molecular interactions. Interestingly, certain molecules such as tannin, lecithin and beta-carotene produced anomalously high positive scores (1600,21 kcal/mol, 134,48 and 556,88 kcal/mol, respectively), suggesting possible limitations in the docking calculations for large, structurally complex molecules that may not fit properly within the binding pocket. Overall, these findings highlight a subset of *Rosa canina* phytochemicals with strong predicted inhibitory potential against tyrosinase, warranting further exploration through *in vitro* assays and pharmacological validation.

The 2D and 3D binding modes of the three molecules (linoleic acid, alpha-tocophenol and oleic acid) with the best docking scores among twenty-five phytochemical molecules obtained from *Rosa canina* are shown in Figure 1. The

molecular docking analysis revealed that linoleic acid establishes a stable interaction within the binding pocket of tyrosinase through a combination of hydrogen bonding and hydrophobic contacts (Figure 1a). The carboxyl group of linoleic acid formed conventional hydrogen bonds with Arg54 and Ile41, anchoring the polar head of the molecule near the entrance of the binding pocket. In addition to these polar interactions, multiple  $\pi$ -alkyl and alkyl interactions were detected between the long hydrocarbon chain of linoleic acid and key residues within the binding pocket, including His53, His189, His193, Trp183, and Val194. These residues, especially the conserved histidines (His53, His189, and His193), are crucial for copper ion and peroxide coordination and enzymatic activity, suggesting that the insertion of linoleic acid into this region could interfere with substrate binding or catalytic turnover. The hydrophobic tail of linoleic acid exhibited extensive van der Waals contacts with the aromatic and aliphatic residues in the binding pocket,

providing structural stabilization despite the molecule's relatively flexible conformation. This combination of hydrogen bonding at the carboxyl end and widespread hydrophobic interactions across the hydrocarbon chain

indicates that linoleic acid may act as a competitive inhibitor, occupying the binding cavity and obstructing access to natural substrates.

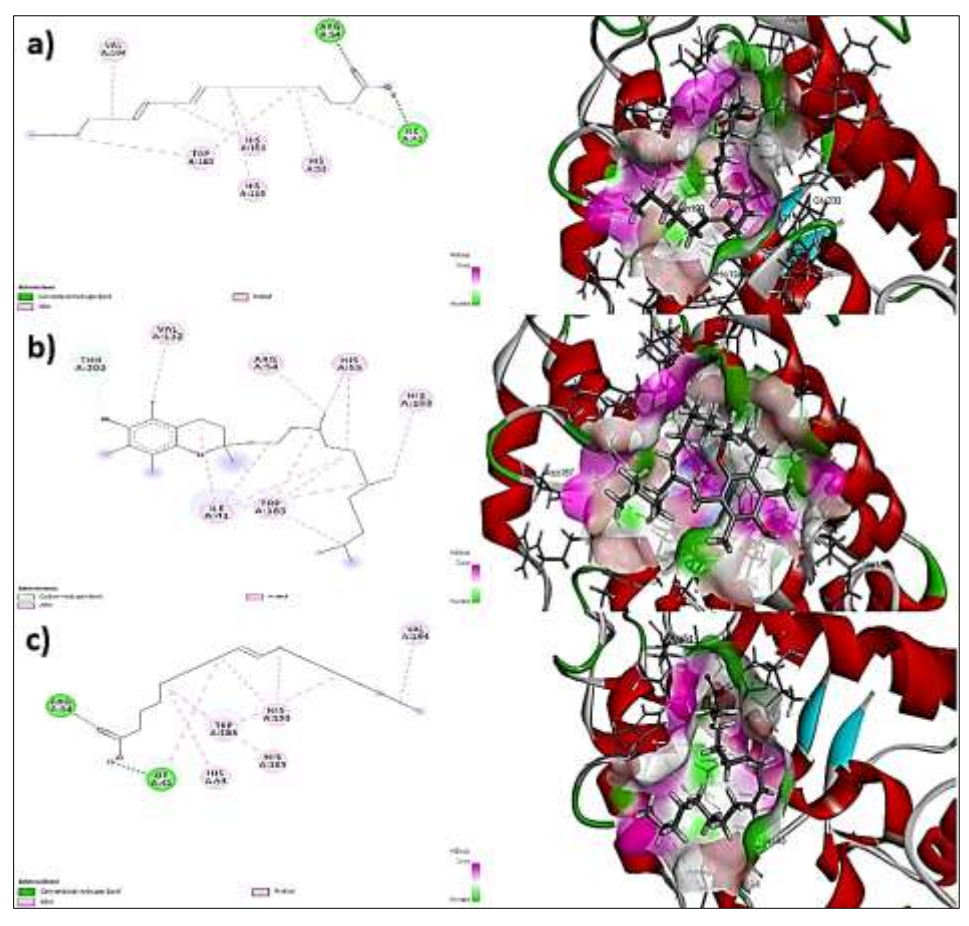


Fig 1: Binding modes of the three active molecules with the best docking scores with tyrosinase enzyme. a-) linoleic acid b-) alpha-tocophenol c-) oleic acid

The docking analysis of alpha-tocopherol with tyrosinase revealed a stable binding mode characterized by multiple hydrophobic and hydrogen bonding interactions. As shown in the Figure 1b, the hydroxyl group of alpha-tocopherol forms a carbon-hydrogen bond with Thr202, which plays a supportive role in molecule stabilization within the binding pocket. In addition, extensive hydrophobic contacts, particularly alkyl and  $\pi$ -alkyl interactions, contribute significantly to the overall binding affinity. Notably, strong  $\pi$ -alkyl interactions are observed with His53, His193, Arg54, Val132, Ile41, and Trp183, residues that are located near the catalytic pocket and are known to be critical for substrate binding and enzymatic function. Collectively, this binding mode suggests that alphatocopherol may exert an inhibitory effect by occupying the binding pocket of tyrosinase and interfering with its catalytic machinery. The docking analysis of oleic acid within the binding pocket of tyrosinase demonstrated a favorable binding orientation stabilized by both hydrogen bonding and hydrophobic interactions (Figure 1c). The carboxyl group of oleic acid formed two conventional hydrogen bonds with Arg54 and Ile41, suggesting a strong anchoring mechanism that positions the molecule firmly within the binding pocket. Beyond these polar contacts, the hydrophobic tail of oleic acid engaged in extensive  $\pi$ -alkyl and alkyl interactions with several key residues, including His53, His189, His193, Trp183, and Val194. The long aliphatic chain of oleic acid allows for optimal hydrophobic complementarity with the non-polar pocket regions, thereby contributing substantially to the overall binding affinity. Taken together, the binding mode of oleic acid highlights a dual stabilizing mechanism through hydrogen bonding and extensive hydrophobic interactions, suggesting its potential role as an effective inhibitor of tyrosinase.

Across the two molecules (linoleic acid and oleic acid) exhibit a convergent binding strategy in tyrosinase whereby the carboxyl group anchors via hydrogen bonds (e.g., Arg54/Ile41) while their long aliphatic chains establish extensive alkyl/ $\pi$ -alkyl contacts with hydrophobic residues near the catalytic histidines, yielding strong predicted affinities. In contrast, alpha-tocopherol is primarily stabilized by a supportive C-H bond with Thr202 and a dense network of  $\pi$ -alkyl interactions (e.g., His53/His193/Trp183), collectively suggesting that all three ligands may inhibit by occupying the pocket and perturbing the catalytic pocket, albeit through complementary polar-hydrophobic versus predominantly hydrophobic-aromatic mechanisms.

#### **ADME** profiles

The pharmacokinetic properties of twenty-five active molecules derived from *Rosa canina* were evaluated using the SwissADME web tool, focusing on gastrointestinal (GI) absorption, blood-brain barrier (BBB) permeability, and cytochrome P450 (CYP) enzyme inhibition profiles (Table 2.).

Table 2: Gastrointestinal absorption, BBB permeability, and CYP inhibition profiles of Rosa canina phytochemicals.

Molecule Name	GI Absorption	BBB permeant	CYP1A2 inhibitor	CYP2C19 inhibitor	CYP2C9 inhibitor	CYP2D6 inhibitor	CYP3A4 inhibitor
Acetic acid	High	No	No	No	No	No	No
Alpha tocophenol	Low	No	No	No	No	No	No
Protocatechuic acid	High	No	No	No	No	No	Yes
Quercitrin	Low	No	No	No	No	No	No
Riboflavin	Low	No	No	No	No	No	No
Thiamin	High	No	No	No	No	No	No
Vanillic acid	High	No	No	No	No	No	No
Vanillin	High	Yes	No	No	No	No	No
Ascorbic acid	High	No	No	No	No	No	No
Beta carotene	Low	No	No	No	No	No	No
Caffeic acid	High	No	No	No	No	No	No
Catechin	High	No	No	No	No	No	No
Citric acid	Low	No	No	No	No	No	No
Epicatechin	High	No	No	No	No	No	No
Ferulic acid	High	Yes	No	No	No	No	No
Gallic acid	High	No	No	No	No	No	Yes
Hyperoside	Low	No	No	No	No	No	No
Isoquercitrin	Low	No	No	No	No	No	No
Lecithin	Low	No	No	No	Yes	No	Yes
Linoleic acid	Low	No	No	No	No	No	No
Oleic acid	High	No	Yes	No	Yes	No	No
P-coumaric acid	High	Yes	No	No	No	No	No
Niacin	High	Yes	No	No	No	No	No
Pectin	Low	No	No	No	No	No	No

The results revealed considerable variability among the molecules in terms of oral bioavailability potential. While several compounds, such as acetic acid, thiamin, vanillic acid, vanillin, ascorbic acid, caffeic acid, catechin, epicatechin, ferulic acid, gallic acid, oleic acid, and niacin, demonstrated high predicted GI absorption, others, particularly glycosylated flavonoids (e.g., quercitrin, hyperoside, isoquercitrin) and macromolecules such as pectin and lecithin, were classified as having low absorption, consistent with their polar or bulky structural features. In terms of BBB permeability, only a limited number of molecules, including vanillin, ferulic acid, p-coumaric acid, and niacin, were predicted to cross the barrier, indicating selective potential for central nervous system (CNS) activity. Regarding metabolic interactions, the majority of molecules were not predicted to inhibit major CYP isoforms, suggesting a relatively low risk of drug-drug interactions. However, exceptions were noted: protocatechuic acid and gallic acid were predicted to inhibit CYP3A4, while oleic acid showed inhibition toward CYP1A2 and CYP2C9, and lecithin was positive for CYP2C9 and CYP3A4 inhibition. These findings indicate that although *Rosa canina* phytochemicals generally possess favorable absorption and low CYP inhibition profiles, their ability to reach systemic circulation and the CNS varies considerably depending on their polarity and structural complexity. Such ADME properties should be taken into account when considering these compounds for therapeutic applications, particularly in the context of oral delivery and potential metabolic interactions.

The drug-likeness and pharmacokinetic profiles of the *Rosa canina* phytochemicals were further assessed through SwissADME predictions, focusing on rule-based filters (Lipinski, Ghose, Veber, Egan, and Muegge), bioavailability scores, and synthetic accessibility (Table 3.).

Table 3: Drug-likeness evaluation, bioavailability scores, and synthetic accessibility of Rosa canina phytochemicals predicted by SwissADME.

Molecule Name	Drug-likeness Filters (Violations)	Bioavailability Score	Synthetic Accessibility	
Acetic acid	Ghose:3, Muegge:2	0.85	1.00	
Alpha tocophenol	Lipinski:1, Veber:1, Egan:1, Muegge:1, Ghose:3	0.55	5.17	
Protocatechuic acid	Ghose:3, Muegge:1	0.56	1.07	
Quercitrin	Lipinski:2, Veber:1, Egan:1, Muegge:3	0.17	5.28	
Riboflavin	Ghose:1, Veber:1, Egan:1, Muegge:1	0.55	3.84	
Thiamin	-	0.55	2.99	
Vanillic acid	Muegge:1	0.85	1.42	
Vanillin	Ghose:2, Muegge:1	0.55	1.15	
Ascorbic acid	Ghose:2, Muegge:1	0.56	3.47	
Beta carotene	Lipinski:1, Veber:1, Egan:1, Muegge:1, Ghose:3	0.55	5.17	
Caffeic acid	Muegge:1	0.56	1.81	
Catechin	-	0.55	3.50	
Citric acid	Ghose:2, Muegge:1, Egan:1	0.56	2.18	
Epicatechin	<del>-</del>	0.55	3.50	
Ferulic acid	Muegge:1	0.85	1.93	
Gallic acid	Ghose:2, Muegge:1	0.56	1.22	
Hyperoside	Lipinski:2, Veber:1, Egan:1, Muegge:3, Ghose:1	0.17	5.32	
Isoquercitrin	Lipinski:2, Veber:1, Egan:1, Muegge:3, Ghose:1	0.17	5.31	
Lecithin	Lipinski:1, Veber:1, Egan:1, Muegge:3, Ghose:4	0.55	7.96	
Linoleic acid	Lipinski:2, Veber:1, Egan:1, Muegge:3, Ghose:1	0.17	5.32	
Oleic acid	Lipinski:1, Veber:1, Egan:1, Muegge:1, Ghose:1	0.85	3.07	
P-coumaric acid	Muegge:1	0.85	1.61	
Niacin	Ghose:3, Muegge:1	0.85	1.00	
Pectin	Ghose:2, Muegge:2	0.56	3.94	

The analysis demonstrated that a considerable proportion of the molecules exhibited multiple violations of drug-likeness filters, particularly glycosylated flavonoids such as quercitrin, hyperoside, isoquercitrin, and lecithin, which showed up to four rule violations, reflecting their high molecular weight (e.g., 758.06 for lecithin and 464.38 for hyperoside), polar surface area (e.g., 218.47 for lecithin and 110.16 for hyperoside), and poor predicted oral bioavailability (scores as low as 0.17). Conversely, smaller phenolic acids (e.g., vanillin, caffeic acid, ferulic acid, p-coumaric acid) and lipophilic molecules (e.g., oleic acid) largely complied with the filters and displayed higher bioavailability scores (0.55-0.85), suggesting better oral absorption potential. Molecules such as acetic acid, ferulic acid, oleic acid, vanillic acid, and niacin reached the highest bioavailability score of 0.85, highlighting their favorable pharmacokinetic characteristics. With respect to synthetic accessibility, most molecules were predicted to be easily synthesizable (scores close to 1.0-3.5), with acetic acid, niacin, and protocatechuic acid being the

most accessible (scores ~1.0). However, certain complex structures such as lecithin (7.96) and quercitrin derivatives (>5.0) were estimated to be synthetically challenging, which may limit large-scale drug development. Taken together, these results suggest that while *Rosa canina* contains several active molecules with promising oral bioavailability and feasible synthetic accessibility, the more complex glycosides display suboptimal drug-likeness and limited drug development potential without structural optimization.

#### Toxicity analysis of phytochemicals

The toxicity profiles of twenty-five *Rosa canina* phytochemicals were predicted using the ProTox 3.0 web server, with outputs expressed as toxicity classes, estimated LD<sub>50</sub> values (mg/kg), average similarity, and prediction accuracy (Table 4.). ProTox 3.0 web server predictions classified the *Rosa canina* phytochemicals into toxicity categories ranging from Class I (fatal if swallowed, LD<sub>50</sub>  $\leq$  5 mg/kg) to Class VI (non-toxic, LD<sub>50</sub>  $\geq$  5000 mg/kg).

**Table 4:** Oral toxicity prediction of *Rosa canina* phytochemicals of by Protox 3.0 web server.

Molecule Name	<b>Predicted Toxicity Class</b>	Predicted LD <sub>50</sub> (mg/kg)	Average Similarity (%)	Prediction Accuracy (%)
Acetic acid	I	333	100.00	100.00
Alpha tocophenol	V	5000	82.25	70.97
Protocatechuic acid	IV	2000	87.23	70.97
Quercitrin	V	5000	97.30	72.90
Riboflavin	VI	10000	82.26	70.97
Thiamin	IV	1000	36.88	23.00
Vanillic acid	IV	2000	79.35	69.26
Vanillin	IV	1000	100.00	100.00
Tannin	V	2500	75.72	69.26
Ascorbic acid	V	3367	100.00	100.00
Beta carotene	IV	1510	83.45	70.97
Caffeic acid	V	2980	88.59	70.97
Catechin	VI	10000	100.00	100.00
Citric acid	III	80	100.00	100.00
Epicatechin	VI	10000	100.00	100.00
Ferulic acid	IV	1772	86.10	70.97
Gallic acid	IV	2000	84.82	70.97
Hyperoside	V	5000	97.30	72.90
Isoquercitrin	V	5000	95.70	72.90
Lecithin	V	3520	61.79	68.07
Linoleic acid	VI	10000	100.00	100.00
Oleic acid	II	48	100.00	100.00
P-coumaric	V	2850	100.00	100.00
Niacin	V	3720	100.00	100.00
Pectin	VI	10000	77.22	69.26

Among the selected molecules, only oleic acid was classified as Class II (LD<sub>50</sub> = 48 mg/kg), indicating a high acute toxicity potential even at low doses. Acetic acid, with an LD<sub>50</sub> of 333 mg/kg, was placed in Class I, corresponding to the 'fatal if swallowed' category. Citric acid (LD<sub>50</sub> = 80 mg/kg) also fell into Class III, suggesting that it poses a considerable toxicity risk when ingested at high concentrations. A substantial number of compounds, including protocatechuic acid, vanillic acid, vanillin, beta carotene, ferulic acid, and gallic acid, were grouped under Class IV (harmful if swallowed; 300 < LD₅0 ≤ 2000 mg/kg). These compounds present moderate toxicity, suggesting that while they may be generally safe at low concentrations, high doses could induce harmful effects. Several phytochemicals such as quercitrin, hyperoside, isoquercitrin, tannin, lecithin, niacin, and ascorbic acid were categorized in Class V (may be harmful if swallowed; 2000 < LD<sub>50</sub> ≤ 5000 mg/kg), reflecting relatively low acute toxicity and compatibility with therapeutic applications. The safest group comprised molecules such as catechin, linoleic acid, riboflavin, epicatechin, and pectin, which were assigned to Class VI (non-toxic;  $LD_{50} > 5000$  mg/kg), supporting their potential as safe bioactive candidates. Overall, these predictions indicate that while most *Rosa canina* phytochemicals fall into low-to-moderate toxicity classes (IV-VI), a few molecules (notably oleic acid, citric acid and acetic acid) exhibit higher toxicity risks and may require cautious dose optimization in pharmacological or nutraceutical applications.

The toxicity profiling of 25 phytochemicals from *Rosa canina* was carried out using the ProTox 3.0 web server, and the results indicated considerable variability in their predicted safety profiles (Table 5.). ProTox 3.0 web server toxicological profiling of the 25 *Rosa canina* phytochemicals reveals a heterogeneous safety landscape and several clear patterns that warrant cautious interpretation and experimental follow-up.

**Table 5:**Toxicological endpoint predictions of the *Rosa canina* phytochemicals estimated using the ProTox 3.0 web server.

Molecule	Hepato	Neuro	Nephro	Respiratory	Cardio	Carsino	Immuno	Muta	Cyto
Name	toxicity	toxicity	toxicity	toxicity	toxicity	genicity	toxicity	genicity	toxicity
Acetic acid	Inactive	Inactive	Inactive	Inactive	Inactive	Inactive	Inactive	Inactive	Inactive
Alpha tocophenol	Inactive	Inactive	Inactive	Active	Inactive	Inactive	Inactive	Inactive	Inactive
Protocatechuic acid	Inactive	Inactive	Active	Inactive	Inactive	Active	Inactive	Inactive	Inactive
Quercitrin	Inactive	Inactive	Active	Active	Active	Active	Active	Inactive	Inactive
Riboflavin	Inactive	Active	Active	Active	Inactive	Inactive	Inactive	Inactive	Inactive
Thiamin	Inactive	Active	Inactive	Active	Inactive	Inactive	Inactive	Inactive	Inactive
Vanillic acid	Inactive	Inactive	Active	Inactive	Inactive	Inactive	Inactive	Inactive	Inactive
Vanillin	Inactive	Inactive	Active	Inactive	Inactive	Inactive	Inactive	Inactive	Inactive
Tannin	Inactive	Inactive	Active	Active	Inactive	Inactive	Active	Inactive	Inactive
Ascorbic acid	Inactive	Inactive	Active	Inactive	Inactive	Inactive	Inactive	Inactive	Inactive
Beta carotene	Inactive	Active	Inactive	Inactive	Inactive	Inactive	Inactive	Active	Inactive
Caffeic acid	Inactive	Inactive	Active	Inactive	Inactive	Active	Inactive	Inactive	Inactive
Catechin	Inactive	Inactive	Active	Active	Inactive	Inactive	Inactive	Inactive	Inactive
Citric acid	Inactive	Inactive	Inactive	Active	Inactive	Inactive	Inactive	Inactive	Inactive
Epicatechin	Inactive	Inactive	Active	Active	Inactive	Inactive	Inactive	Inactive	Inactive
Ferulic acid	Inactive	Inactive	Active	Inactive	Inactive	Inactive	Active	Inactive	Inactive
Gallic acid	Inactive	Inactive	Active	Active	Inactive	Active	Inactive	Inactive	Inactive
Hyperoside	Inactive	Inactive	Active	Active	Inactive	Inactive	Active	Inactive	Inactive
Isoquercitrin	Inactive	Inactive	Active	Active	Inactive	Active	Active	Inactive	Inactive
Lecithin	Inactive	Inactive	Active	Active	Inactive	Inactive	Active	Inactive	Inactive
Linoleic acid	Inactive	Inactive	Inactive	Inactive	Inactive	Inactive	Inactive	Inactive	Inactive
Oleic acid	Inactive	Inactive	Inactive	Inactive	Inactive	Inactive	Inactive	Inactive	Inactive
P-coumaric acid	Inactive	Inactive	Active	Inactive	Inactive	Active	Inactive	Inactive	Inactive
Niacin	Active	Active	Active	Active	Inactive	Inactive	Inactive	Inactive	Inactive
Pectin	Inactive	Inactive	Active	Inactive	Inactive	Inactive	Inactive	Inactive	Inactive

Among the analyzed molecules, only three (acetic acid, linoleic acid, and oleic acid) were consistently predicted as 'inactive' across all assessed toxicity endpoints, suggesting a relatively favorable in silico safety profile according to the ProTox 3.0 web server predictions. By contrast, nephrotoxicity emerges as the most frequently predicted liability, affecting a large proportion of the dataset (e.g., protocatechuic acid, quercitrin, riboflavin, vanillic acid, vanillin, tannin, ascorbic acid, caffeic acid, catechin, epicatechin, ferulic acid, gallic acid, hyperoside, isoquercitrin, lecithin, p-coumaric acid and pectin), which indicates a recurring structural or mechanistic feature in these molecules that the model associates with renal risk. Respiratory toxicity is also commonly predicted (including alpha-tocopherol, quercitrin, riboflavin, thiamin, tannin, catechin, citric acid, epicatechin, gallic acid, hyperoside, isoquercitrin and lecithin), whereas neurotoxicity predictions are relatively uncommon (riboflavin, thiamin, beta-carotene and niacin). A smaller subset of compounds is flagged for immunotoxicity (e.g., quercitrin, tannin, ferulic acid, hyperoside, isoquercitrin and lecithin) and carcinogenicity (protocatechuic acid, quercitrin, caffeic acid, gallic acid, isoquercitrin and pcoumaric acid). Only quercitrin was predicted to present a cardiotoxicity concern in this dataset, and niacin is the sole compound flagged for hepatotoxicity; importantly, none of the tested molecules were predicted cytotoxic by ProTox 3.0 web server in the supplied output.

# Conclusion

This study systematically profiled 25 Rosa canina phytochemicals as prospective tyrosinase modulators through an integrated pipeline curation from Dr. Duke's database, ligand optimization, target preparation (PDB: 1WX2), PLANTS docking at a defined binding pocket, and ADME and toxicity filtering. Three molecules exhibited the most favorable binding affinities in the docking stage: linoleic acid (-89.79 kcal/mol), alpha-tocopherol (-89.58 kcal/mol) and

oleic acid (-83.82 kcal/mol). Binding mode inspection indicated a shared anchoring motif for the two fatty acids (oleic acid and linoleic acid) hydrogen bonds to Arg54 and Ile41 (together with extensive alkyl/ $\pi$ ) alkyl contacts to hydrophobic residues near the conserved histidines (His53, His189, His193). By contrast, alpha-tocopherol relied on a supportive C-H interaction with Thr202 plus dense hydrophobic contacts around the catalytic region. These complementary polar-hydrophobic (fatty acids) versus predominantly hydrophobic-aromatic (alpha-tocopherol) mechanisms plausibly account for the favorable docking energies and point to competitive occupation of the catalytic pocket as a putative binding mode. SwissADME predictions revealed that small phenolic acids and oleic acid possessed high gastrointestinal absorption, whereas glycosylated flavonoids (e.g., quercitrin, hyperoside, isoquercitrin) and macromolecular constituents (e.g., hyperoside, lecithin) exhibited poor absorption, consistent with their elevated polarity and molecular size. Most compounds were not predicted to inhibit major CYP isoforms; however, oleic acid (CYP1A2, CYP2C9), protocatechuic acid and gallic acid (CYP3A4), and lecithin (CYP2C9, CYP3A4) emerged as exceptions, highlighting potential drug-drug interaction risks under conditions of systemic exposure. Drug-likeness filters also favored simpler scaffolds (e.g., oleic acid), whereas multiple rule violations and low bioavailability scores for the glycosides suggest limited oral developability without structural optimization or alternative delivery strategies. Toxicity predictions drew a nuanced safety landscape. Acute toxicity classes spanned I-VI, with oleic acid (Class II; LD<sub>50</sub>  $\approx$ 48 mg/kg) and acetic acid (Class I; LD<sub>50</sub>  $\approx$  333 mg/kg) flagged as higher-concern outliers, whereas catechin, epicatechin, linoleic acid, riboflavin, pectin populated the Class hazardous VI. Organ-specific (hepatotoxicity, neurotoxicity, nephrotoxicity, respiratory, cardio, carcinogenicity, immunotoxicity, mutagenicity, cytotoxicity) identified nephrotoxicity as the most common

alert among polyphenolic scaffolds, while acetic acid, linoleic acid, and oleic acid were predicted inactive across all such endpoints. The divergence between acute class assignments and organ inactivities (e.g., for oleic and acetic acids) underscores the model- and endpoint-specific nature of these predictions and the need for experimental corroboration under intended routes, doses, and formulations.

Taken together, linoleic acid, oleic acid, and alpha-tocopherol emerge as the most promising *R. canina* phytochemicals based on binding affinities; however, the predicted CYP interactions of oleic acid and its acute toxicity classification warrant careful consideration in terms of context, dosing, and formulation strategies. Conversely, large and polar glycosides (e.g., quercitrin, hyperoside, isoquercitrin), despite favorable docking profiles, exhibit poor oral drug-likeness and recurrent toxicity flags, suggesting that strategies such as structural simplification toward their aglycones, prodrug or topical delivery, or deprioritization may be more appropriate. The anomalous positive docking scores observed for very large or flexible molecules (e.g., tannin, lecithin, beta-carotene) may reflect the limitations of rigid receptor docking when applied to large ligands.

In summary, by coupling structure-based screening with ADME-toxicity filters, this work narrows a chemically diverse rosehip phytochemical space to a small set of mechanistically plausible, formulation-amenable candidates for tyrosinase modulation. The combined evidence positions linoleic acid,  $\alpha\text{-tocopherol},$  and oleic acid as priorities for experimental validation, while providing actionable guidance on exposure route, interaction risks, and safety hypotheses that can be tested to accelerate their advancement toward cosmeceutical or therapeutic applications targeting melanogenesis.

#### **Declarations**

#### **Conflict of interest**

The authors declare that there are no conflicts of interest.

#### **Compliance with Ethical Standards**

This article does not contain any studies involving human or animal subjects.

#### References

- Kubczak M, Khassenova AB, Skalski B, Michlewska S, Wielanek M, Aralbayeva AN, et al. Bioactive compounds and antiradical activity of the Rosa canina L. leaf and twig extracts. Agronomy. 2020;10(12):1897. doi:10.3390/agronomy10121897.
- 2. Negrean OR, Farcas AC, Nemes SA, Cic DE, Socaci SA, *et al.* Recent advances and insights into the bioactive properties and applications of *Rosa canina* L. and its byproducts. Heliyon. 2024;10(9):e30816. doi:10.1016/j.heliyon.2024.e30816.
- 3. Chrubasik C, Roufogalis BD, Müller-Ladner U, Chrubasik S. A systematic review on the *Rosa canina* effect and efficacy profiles. Phytotherapy Research. 2008;22(6):725-33. doi:10.1002/ptr.2400.
- Stanković MI, Savić VL, Živković JV, Stanojević LP, Tadić VM, Arsić IA. Tyrosinase inhibitory and antioxidant activity of wild *Rosa canina* L. and *Sorbus* aucuparia L. fruit extracts. Acta Poloniae Pharmaceutica-Drug Research. 2019;76(3):523-33. doi:10.32383/appdr/103431.
- Subaş T, Özgen U, Kanbolat Ş, Badem M, Uzuner U, Özdemir G, et al. Bioactive compounds from Rosa

- *canina* L. roots with anti-collagenase, anti-tyrosinase, and antioxidant activities: *In vitro* and in silico approaches. Chemistry & Biodiversity. 2025;22:e00357. doi:10.1002/cbdv.202500357.
- Lemoni Z, Kalantzi S, Lymperopoulou T, Tzani A, Stavropoulos G, Detsi A, et al. Kinetic modeling and biological activities of Rosa canina L. pseudo-fruit extracts obtained via enzyme-assisted extraction. Antioxidants. 2025;14(5):558. doi:10.3390/antiox14050558.
- 7. Kanteev M, Goldfeder M, Fishman A. Structure-function correlations in tyrosinases. Protein Science. 2015;24(9):1360-9. doi:10.1002/pro.2734.
- 8. Ito S, Sugumaran M, Wakamatsu K. Chemical reactivities of ortho-quinones produced in living organisms: Fate of quinonoid products formed by tyrosinase and phenoloxidase action on phenols and catechols. International Journal of Molecular Sciences. 2020;21(17):6080. doi:10.3390/ijms21176080.
- 9. Chang TS. An updated review of tyrosinase inhibitors. International Journal of Molecular Sciences. 2009;10(6):2440-75. doi:10.3390/ijms10062440.
- 10. Wu Q, Fang W, Liu H, Liu Z, Xu X. *Rosa* × *damascena* Herrm. essential oil: anti-tyrosinase activity and phytochemical composition. Frontiers in Pharmacology. 2024;15:1451452. doi:10.3389/fphar.2024.1451452.
- 11. Yoruk R, Marshall MR. Physicochemical properties and function of plant polyphenol oxidase: a review. Journal of Food Biochemistry. 2003;27(5):361-422.
- 12. Parvez S, Kang M, Chung HS, Cho C, Hong MC, Shin MK, *et al.* Survey and mechanism of skin depigmenting and lightening agents. Phytotherapy Research. 2006;20(11):921-34. doi:10.1002/ptr.1954.
- 13. Kim YJ, Uyama H. Tyrosinase inhibitors from natural and synthetic sources: structure, inhibition mechanism and perspective for the future. Cellular and Molecular Life Sciences (CMLS). 2005;62(15):1707-23. doi:10.1007/s00018-005-5054-y.
- 14. Loizzo MR, Tundis R, Menichini F. Natural and synthetic tyrosinase inhibitors as antibrowning agents: an update. Comprehensive Reviews in Food Science and Food Safety. 2012;11(4):378-98. doi:10.1111/j.1541-4337.2012.00191.x.
- 15. Pinzi L, Rastelli G. Molecular docking: shifting paradigms in drug discovery. International Journal of Molecular Sciences. 2019;20(18):4331. doi:10.3390/ijms20184331.
- Morris GM, Lim-Wilby M. Molecular docking. In: Molecular Modeling of Proteins. Totowa (NJ): Humana Press; 2008. p. 365-82. doi:10.1007/978-1-59745-177-2\_19.
- 17. Daina A, Michielin O, Zoete V. SwissADME: a free web tool to evaluate pharmacokinetics, drug-likeness and medicinal chemistry friendliness of small molecules. Scientific Reports. 2017;7:42717. doi:10.1038/srep42717.
- 18. Banerjee P, Kemmler E, Dunkel M, Preissner R. ProTox 3.0: a webserver for the prediction of toxicity of chemicals. Nucleic Acids Research. 2024;52(W1):W513-20. doi:10.1093/nar/gkae303.
- 19. Duke JA. Handbook of Phytochemical Constituents of GRAS Herbs and Other Economic Plants. Boca Raton (FL): CRC Press; 1992.

- 20. Kim S, Chen J, Cheng T, Gindulyte A, He J, He S, *et al.* PubChem 2025 update. Nucleic Acids Research. 2025;53(D1):D1516-25. doi:10.1093/nar/gkae1059.
- 21. Hanwell MD, Curtis DE, Lonie DC, Vandermeersch T, Zurek E, Hutchison GR. Avogadro: an advanced semantic chemical editor, visualization, and analysis platform. Journal of Cheminformatics. 2012;4:17. doi:10.1186/1758-2946-4-17.
- 22. Matoba Y, Kumagai T, Yamamoto A, Yoshitsu H, Sugiyama M. Crystallographic evidence that the dinuclear copper center of tyrosinase is flexible during catalysis. Journal of Biological Chemistry. 2006;281(13):8981-90. doi:10.1074/jbc.M509785200.
- 23. Burley SK, Bhikadiya C, Bi C, Bittrich S, Chen L, Crichlow GV, *et al.* RCSB Protein Data Bank: celebrating 50 years of the PDB with new tools for understanding and visualizing biological macromolecules in 3D. Protein Science. 2022;31(1):187-208. doi:10.1002/pro.4213.
- 24. Pettersen EF, Goddard TD, Huang CC, Couch GS, Greenblatt DM, Meng EC, *et al.* UCSF Chimera—a visualization system for exploratory research and analysis. Journal of Computational Chemistry. 2004;25(13):1605-12. doi:10.1002/jcc.20084.
- 25. Exner TE, Korb O, Ten Brink T. New and improved features of the docking software PLANTS. Chemistry Central Journal. 2009;3(Suppl 1):P16. doi:10.1186/1752-153X-3-S1-P16.
- BIOVIA Dassault Systèmes. BIOVIA Discovery Studio Visualizer 2020. San Diego (CA): Dassault Systèmes; 2020